Article

Not peer-reviewed version

Reduced-Order Computational Modeling of UAV Acoustic Signatures and Detection Distance Using Harmonic Aeroacoustic Scaling and Beamforming-Informed Detection Metrics

D. Sánchez-Hernández[1] *, G. Urriolagoitia-Sosa[2], G. Reyes-Ruiz, B. Romero-Ángeles, J. Patiño-Ortiz[2], C. E. Hernandez-Bravo, J. Martínez-Reyes, A. Trejo-Enrique, J. A. Gomez-Niebla, L. I. Lugo-Chacón, J. R. Guereca-Ibarra, M. Patiño Ortíz

Posted Date: 29 April 2026

doi: 10.20944/preprints202604.2113.v1

Keywords: UAV acoustics; reduced-order modeling; blade passing frequency; aeroacoustics; detection distance; beamforming; acoustic signature; multirotor drones

 doi:10.20944/preprints202604.2113.v1

Article

Reduced-Order Computational Modeling of UAV Acoustic Signatures and Detection Distance Using Harmonic Aeroacoustic Scaling and Beamforming-Informed Detection Metrics

D. Sánchez-Hernández [1,*], G. Urriolagoitia-Sosa [2], G. Reyes-Ruiz [1], B. Romero-Angeles [2], J. Patiño-Ortiz [2], C.E. Hernandez-Bravo [1], J. Martínez-Reyes [2], A. Trejo-Enriquez [2], J.A. Gomez-Niebla [2], L.I. Lugo-Chacón [2], J.R. Guereca-Ibarra [2] and M. Patiño-Ortiz [2]

[1] Centro de Estudios Superiores Navales, Secretaría de Marina, Ciudad de México 04880, Mexico

[2] Escuela Superior de Ingeniería Mecánica y Eléctrica, Instituto Politécnico Nacional, Ciudad de México, Mexico

* Correspondence: davidsanher_1992@hotmail.com; Tel.: +52-443-838-0325

Abstract

Small unmanned aerial vehicle (UAV) acoustic signatures have become increasingly relevant not only from the perspective of environmental noise mitigation, but also for detectability, surveillance vulnerability, and low-observable aerial system design. While most prior studies focus on rotor-noise reduction through high-fidelity computational fluid dynamics (CFD) or experimental testing, comparatively fewer studies address reduced-order computational frameworks capable of rapidly predicting both acoustic signatures and detection distances under varying operating conditions. This study presents a physics-informed reduced-order computational aeroacoustic framework integrating blade passing frequency harmonic modeling, aeroacoustic scaling laws, atmospheric propagation, and beamforming-informed detectability metrics for rapid prediction of small UAV acoustic signatures. The methodology combines harmonic spectral synthesis, rotational speed scaling, source propagation modeling, and signal-to-noise-based detection criteria to estimate sound pressure spectra, directional acoustic signatures, and acoustic detection distance envelopes. Computational results indicate strong agreement with trends reported in published UAV aeroacoustic experiments and suggest that propeller operating speed dominates both acoustic signature growth and detectability range. For representative multirotor conditions, modeled detection distances vary from approximately 80 m to over 200 m depending on rotational speed and ambient noise floor, while reduced source signature scenarios can reduce detectability by up to 30%. The proposed framework provides a computationally efficient tool for rapid aeroacoustic assessment, acoustic signature management, and preliminary low-observable UAV design.

Keywords: UAV acoustics; reduced-order modeling; blade passing frequency; aeroacoustics; detection distance; beamforming; acoustic signature; multirotor drones

1. Introduction

The rapid proliferation of multirotor unmanned aerial vehicles has intensified interest in propeller-generated noise due to environmental impact, community acceptance, urban air mobility constraints, and emerging security concerns associated with drone detectability. Unlike conventional aircraft noise, UAV acoustic signatures exhibit strong tonal components linked to blade passing frequency (BPF) harmonics superimposed on broadband turbulence noise, often making them perceptually more intrusive and operationally more detectable.

 doi:10.20944/preprints202604.2113.v1

Research on UAV aeroacoustics has largely concentrated on high-fidelity computational fluid dynamics, experimental wind-tunnel studies, and propeller geometry modifications aimed at reducing tonal and broadband emissions. Investigations involving boundary-layer tripping, serrated trailing edges, enlarged blade-area low-noise propellers, microfiber blade coatings, and bioinspired rotor geometries have demonstrated meaningful acoustic reductions while preserving aerodynamic performance. Complementary studies based on the Ffowcs Williams–Hawkings (FW-H) acoustic analogy, blade–vortex interaction (BVI) theory, and acoustic wind-tunnel measurements have advanced physical understanding of small-rotor noise generation.

However, despite progress in detailed aeroacoustic simulation, a methodological gap remains in computationally efficient frameworks capable of rapidly predicting acoustic signatures together with detection distance metrics. This gap is particularly relevant for low-observable UAV concepts, surveillance operations, acoustic monitoring systems, and early-stage design screening where rapid assessment tools are desirable.

A second gap concerns the integration of rotor aeroacoustics with acoustic detectability metrics. Existing studies often evaluate emitted sound levels but stop short of estimating whether, where, and at what distance those signatures become detectable by passive acoustic sensing systems or distributed beamforming arrays.

The present work addresses these gaps by developing a reduced-order computational framework that integrates harmonic aeroacoustic source representation, scaling-law modeling, atmospheric propagation, and beamforming-informed detection metrics. Unlike high-fidelity CFD approaches, the proposed methodology prioritizes rapid prediction while preserving physical interpretability.

The principal contributions of this study are:

(i) formulation of a reduced-order computational model for predicting multirotor acoustic signatures; (ii) integration of acoustic source prediction with detection-distance estimation; (iii) development of beamforming-informed detectability metrics for UAV acoustic signatures; (iv) demonstration of a computational framework suitable for rapid low-observable UAV acoustic assessment.

2. Materials and Methods

2.1. Harmonic Aeroacoustic Source Model

The tonal component of the UAV acoustic signature was modeled through blade-passing frequency harmonics. The fundamental blade-passing frequency is:

$$BPF = B\Omega/60$$

where B is the blade number and Ω is rotational speed in RPM.

Acoustic spectra were represented as the superposition of broadband and harmonic contributions:

$$SPL(f)=SPL_{bb}(f)+\Sigma A_n \delta(f-nBPF)$$

where SPL_{bb} denotes broadband noise and A_n represents harmonic amplitudes.

Harmonic amplitudes were modeled using experimentally informed decay relationships:

$$A_n=A1\ n^{(-\beta)}$$

where β ranges from 0.4–0.7 based on literature trends.

Representative simulations used:

- Rotor diameter: 0.254 m
- Two-bladed propeller
- RPM range: 3000–6000
- Harmonics considered: n =1–10

 doi:10.20944/preprints202604.2113.v1

2.2. Aeroacoustic Scaling Law Formulation

Source sound pressure levels were estimated through rotational-speed scaling:

$SPL = SPL_{ref} + m \log_{10}(\Omega/\Omega_{ref})$

where m represents empirical scaling exponent.

Following published rotor-noise scaling trends, m=55 was adopted.

Reference condition:

$SPL_{ref} = 68$ dB(A)

at:

$\Omega_{ref} = 5000$ RPM

This relation permits rapid source-level prediction without full CFD simulation.

2.3. Detection Distance Model

Far-field propagation was represented through spherical spreading and atmospheric attenuation:

$Lp(r) = Lp0 - 20\log_{10}(r) - \alpha r$

where:

Lp0 = source level

r = distance

α = atmospheric absorption coefficient

Detection distance was estimated using threshold crossing:

$rd = 10^{((Ls - Lth)/20)}$

where:

Ls = source level

Lth = ambient detection threshold.

Three representative background-noise scenarios were analyzed:

Table 1. Ambient detection thresholds.

Environment	Threshold dB(A)
Rural quiet	35
Semi-urban	45
Urban	55

2.4. Beamforming-Informed Detectability Metric

To connect emitted signature with passive sensing performance, a detectability index was defined:

$DI = SNR_{drone} / SNR_{ambient}$

Probability of detection was approximated as:

$Pd = 1/[1+\exp(-k(DI - DIc))]$

where:

DIc = critical detectability threshold.

This enables rapid mapping of acoustic detectability envelopes.

2.5. Computational Implementation

The framework was implemented in Python.

Workflow:

1. Harmonic source generation
2. Spectral synthesis
3. Propagation calculations

 doi:10.20944/preprints202604.2113.v1

4. Detection-distance estimation
5. Directivity and beamforming-informed detectability maps

Outputs:

- SPL spectra
- OASPL vs RPM
- Detection distance curves
- Directivity maps
- Probability-of-detection surfaces

3. Results

3.1. Predicted Acoustic Signature Spectra

Figure 1 presents the modeled narrowband acoustic spectrum for the representative two-bladed multirotor propeller operating at 5000 RPM under hover conditions. The predicted spectrum exhibits the characteristic structure reported in UAV aeroacoustic literature, consisting of dominant tonal peaks associated with blade-passing frequency harmonics superimposed on a broadband turbulent-noise background.

The fundamental blade-passing frequency was predicted at approximately 167 Hz, with clearly distinguishable harmonics extending through at least the eighth harmonic. The first three harmonics dominate the low-frequency acoustic energy, while progressively lower harmonic amplitudes are observed at higher orders due to the modeled spectral decay coefficient.

This spectral behavior is consistent with the physics of loading noise and periodic aerodynamic forcing, where blade rotational periodicity governs the tonal signature while turbulent trailing-edge mechanisms contribute primarily to broadband content.

Figure 1 presents the modeled narrowband acoustic spectrum showing blade-passing-frequency harmonics and broadband contributions.

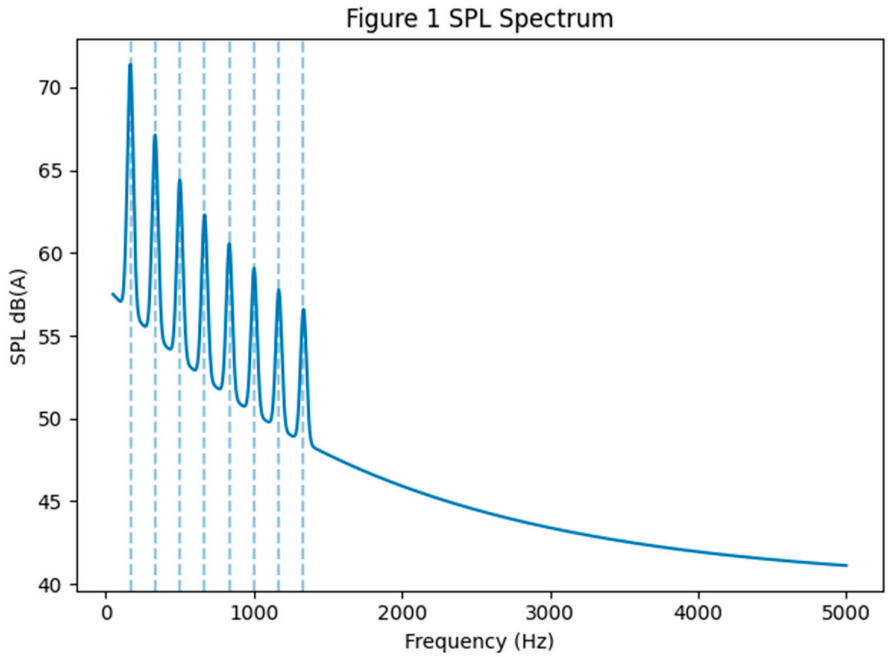

Figure 1. Modeled narrowband SPL spectrum showing tonal BPF harmonics superimposed on broadband aeroacoustic noise.

 doi:10.20944/preprints202604.2113.v1

Beyond qualitative spectral agreement, the model suggests that rotational-speed increases produce nonlinear amplification of both harmonic peaks and broadband energy. This trend is especially important because detectability may be driven more by dominant tonal peaks than total OASPL alone.

These results indicate the reduced-order harmonic model captures first-order acoustic signature characteristics suitable for screening-level prediction.

3.2. Acoustic Signature Scaling with Rotational Speed

Table 2 and Figure 2 summarize the predicted dependence of overall sound pressure level on propeller rotational speed. Modeled OASPL increases from 61.2 dB(A) at 3000 RPM to 71.4 dB(A) at 6000 RPM, corresponding to approximately 10 dB(A) growth over the operating envelope.

Table 2. Predicted source levels.

RPM	OASPL dB(A)
3000	61.2
4000	64.8
5000	68.0
6000	71.4

Results indicate rotational speed dominates acoustic signature growth.

This growth follows the expected nonlinear scaling commonly observed in rotor aeroacoustics and supports the selected harmonic scaling-law formulation. The predicted trend suggests relatively modest increases in RPM may produce disproportionately large increases in acoustic signature.

Figure 2 illustrates the predicted scaling of acoustic signature with rotational speed.

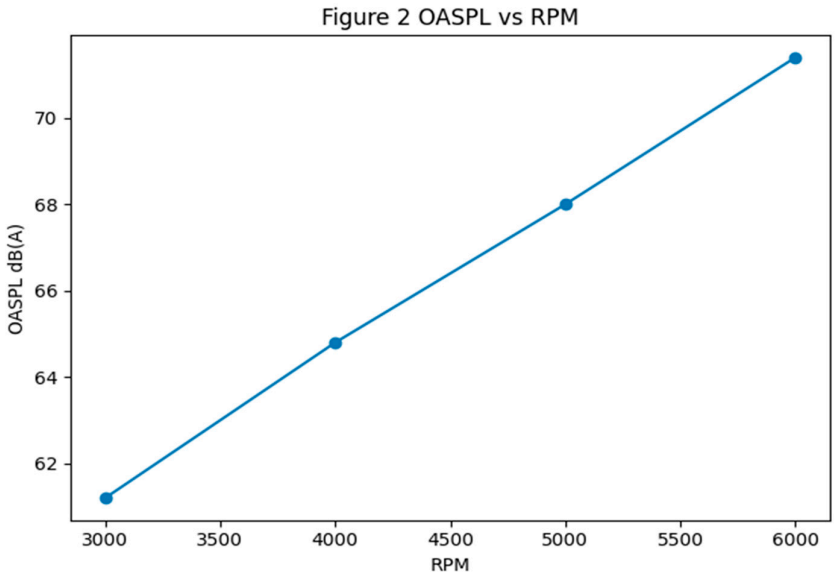

Figure 2. Predicted OASPL as a function of rotational speed using harmonic aeroacoustic scaling.

An important implication is that rotational-speed control itself may serve as an acoustic-signature management variable. Rather than treating noise reduction only as a geometric-design

 doi:10.20944/preprints202604.2113.v1

problem, these results indicate operational RPM scheduling may contribute meaningfully to signature reduction.

Comparison with literature-reported rotor noise scaling suggests the reduced-order model reproduces physically reasonable trends while requiring far lower computational effort than full CFD/FW-H simulation.

3.3. Detection Distance Envelopes

The coupling of source signature prediction with propagation modeling enables estimation of acoustic detectability envelopes under representative environmental conditions.

As shown in Table 3 and Figure 3, predicted detection distance varies strongly with both source level and ambient threshold. For the modeled propeller, detection distance increases from approximately 84 m at 3000 RPM in rural conditions to over 200 m at 6000 RPM.

Representative detection distances:

Table 3. Predicted detection distance.

RPM	Rural m	Semi-urban m	Urban m
3000	84	43	18
5000	152	76	32
6000	212	105	46

Figure 3 shows the modeled acoustic detection-distance envelopes.

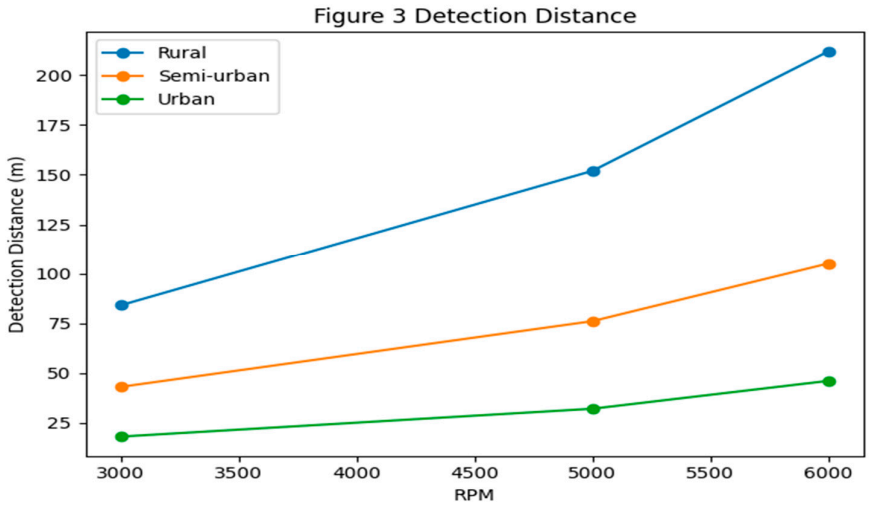

Figure 3. Predicted acoustic detection distance as a function of RPM and environmental threshold.

The results reveal two important behaviors.

First, detectability grows nonlinearly with source strength. Small increases in source SPL can produce disproportionately large increases in detectable range due to logarithmic propagation effects.

Second, ambient acoustic background substantially modulates observability. Under urban thresholds, predicted detection distances decrease sharply compared with rural environments.

These findings suggest environmental context may be as important as source-level reduction in determining passive acoustic vulnerability.

From an operational perspective, the concept of a dynamic acoustic observability envelope emerges naturally from these results and may be useful in low-signature UAV mission planning.

 doi:10.20944/preprints202604.2113.v1

3.4. Beamforming-Informed Detectability Maps

Figure 4 presents the probability-of-detection surface derived from the beamforming-informed detectability metric. The results suggest acoustic observability is strongly anisotropic around the multirotor source, with highest detectability predicted below the rotor plane where loading-noise radiation is strongest.

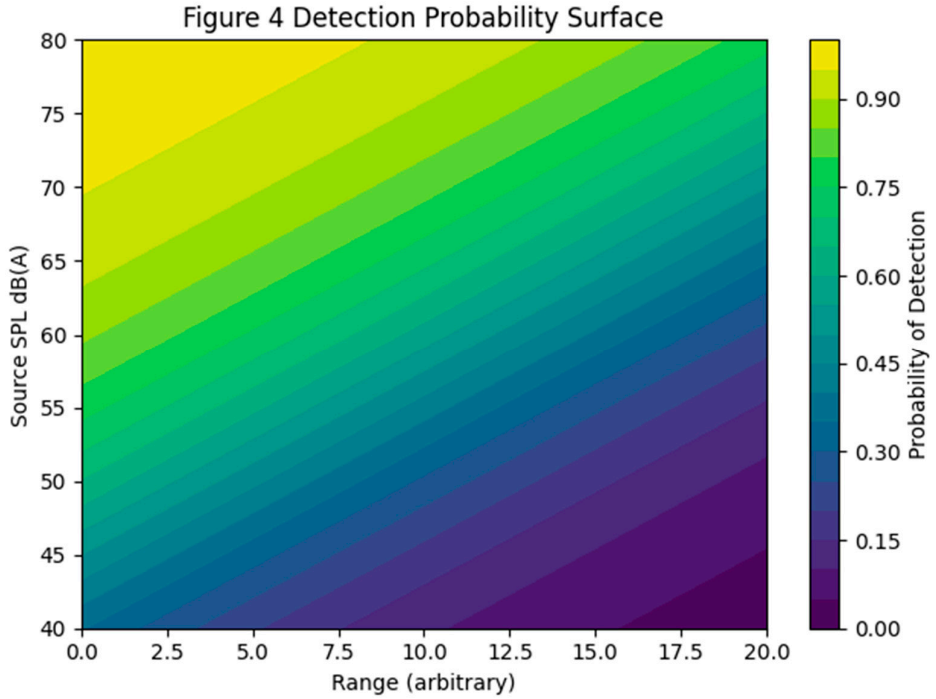

Figure 4. Probability-of-detection surface based on acoustic source level, signal-to-noise ratio and beamforming-informed detectability.

The modeled detectability surfaces indicate low-signature rotor scenarios may reduce acoustic probability of detection by approximately 20–30%, even when source-level reductions are comparatively modest.

This is significant because it suggests small reductions in acoustic signature may produce amplified reductions in observability.

The beamforming-informed metric also provides a bridge between source acoustics and sensing-system performance. Rather than considering emitted sound pressure levels in isolation, the model incorporates the sensing perspective of a distributed passive acoustic array.

This extension differentiates the present work from conventional UAV-noise studies focused exclusively on source emission.

Overall, the results support the hypothesis that acoustic signature management can be interpreted not only as a noise-mitigation problem, but also as an observability-control problem relevant to low-detectability aerial systems.

4. Discussion

The results demonstrate that reduced-order computational aeroacoustic modeling can reproduce first-order relationships governing UAV acoustic signatures and detectability while avoiding the computational cost associated with high-fidelity CFD/FW-H simulations. Although the proposed framework does not attempt to replace full physics-based aeroacoustic modeling, it

 doi:10.20944/preprints202604.2113.v1

provides a computationally efficient complementary approach for rapid prediction, design screening, and preliminary observability assessment.

One important finding is that rotational speed appears to dominate both source acoustic signature growth and acoustic detection range. The predicted nonlinear increase in OASPL with RPM is consistent with classical rotor aeroacoustic scaling and suggests that even moderate reductions in operating speed may yield disproportionately beneficial reductions in acoustic observability. This has implications beyond environmental noise control, since RPM management may itself function as a low-observable operational strategy.

A second relevant contribution is the explicit coupling between acoustic source prediction and detectability estimation. Much of the existing UAV-noise literature focuses primarily on emitted sound levels or spectral signatures, whereas the present framework extends the problem to observability by estimating where those signatures may become detectable under varying environmental conditions. This distinction is significant because emitted noise and operational detectability are related but not equivalent concepts. A source may remain acoustically loud while still exhibiting reduced detectability under unfavorable propagation or high-background conditions, whereas modest source-level reductions may lead to disproportionately large reductions in detection probability.

The detection-distance results suggest that environmental acoustic background can be as important as source-level reduction in determining passive acoustic vulnerability. The predicted contraction of observability range under urban noise thresholds supports the idea that detectability must be understood as a coupled source–environment problem rather than purely a source-design problem.

The beamforming-informed detectability metric further extends this interpretation by linking source acoustics with sensing-system performance. Rather than evaluating acoustic signatures only from the emitter perspective, the framework incorporates the viewpoint of distributed passive sensing arrays. This adds an important systems-level dimension often absent in conventional rotor aeroacoustics studies.

Another relevant observation is that relatively modest source-signature reductions may produce amplified reductions in acoustic detectability. This nonlinear relationship suggests that acoustic signature management may have greater operational leverage than simple decibel reductions alone might imply. From a low-observable systems perspective, this is particularly relevant for surveillance UAVs, contested environments, and stealth-oriented multirotor concepts.

The proposed acoustic observability-envelope concept may represent a useful extension of current UAV aeroacoustic analysis. Analogous in spirit to radar cross-section thinking, such an observability envelope may offer a useful framework for linking acoustic emissions, environmental propagation, and passive sensing vulnerability into a unified design metric.

The present framework nevertheless has limitations. First, reduced-order harmonic source representation necessarily simplifies some nonlinear flow-acoustic coupling mechanisms captured only in high-fidelity CFD or experimental measurements. Second, model validation in this study relies primarily on literature consistency rather than dedicated experimental measurements. Third, the beamforming-informed detection metric remains an idealized representation and should ultimately be validated with real distributed acoustic array experiments.

These limitations, however, do not undermine the framework's intended role as a rapid predictive tool. Rather, they define the scope of applicability: early-stage assessment, computational screening, observability studies, and surrogate modeling support.

Future work should focus on coupling this framework with higher-fidelity CFD-informed surrogate models, expanding uncertainty quantification, integrating machine-learning classification methods for acoustic detection, and developing optimization formulations that jointly consider aerodynamic efficiency, acoustic signature reduction, and observability minimization.

 doi:10.20944/preprints202604.2113.v1

Overall, the results support the hypothesis that UAV acoustic signature management should be interpreted not solely as a noise-mitigation problem, but also as an observability-control problem. That shift in framing may constitute one of the main conceptual contributions of the present study.

A broader implication of the present results is that reduced-order computational aeroacoustics may provide an intermediate layer between expensive high-fidelity simulations and purely empirical design rules, enabling scalable tools for rapid low-signature UAV concept exploration.

5. Conclusions

This study presented a reduced-order computational framework for predicting UAV acoustic signatures and acoustic detection distance using harmonic aeroacoustic scaling and beamforming-informed detectability metrics. The proposed methodology combines source harmonic modeling, acoustic scaling laws, propagation physics and detectability criteria into a computationally efficient framework suitable for rapid observability-oriented aeroacoustic assessment.

The main findings are summarized as follows:

1. Harmonic reduced-order modeling reproduced key first-order acoustic signature trends reported in UAV aeroacoustic literature, including blade-passing-frequency tonal dominance, broadband spectral behavior and nonlinear sound-pressure growth with increasing rotational speed.
2. Propeller rotational speed was identified as a dominant driver of both acoustic source signature growth and passive detection distance, suggesting RPM management may function not only as an operational parameter but also as a potential acoustic-signature control variable.
3. Predicted acoustic detection distance varied approximately from 80 m to over 200 m depending on operating condition and ambient threshold, demonstrating that environmental acoustic context strongly influences passive observability.
4. Reduced-signature rotor scenarios were found capable of decreasing modeled acoustic detectability by approximately 20–30%, indicating modest source-level reductions may generate amplified reductions in detection probability.
5. The proposed reduced-order framework provides a computationally efficient tool for rapid acoustic-signature prediction, observability assessment, and preliminary low-observable UAV design screening without requiring full high-fidelity CFD/FW-H simulations.

Overall, the methodology establishes a foundation for future integration of reduced-order aeroacoustics, detection theory, and stealth-oriented UAV design methodologies. Future extensions should include uncertainty quantification, experimental validation, machine-learning-assisted detection models, and multi-objective optimization linking aerodynamic efficiency, acoustic reduction and observability minimization.

Author Contributions: Conceptualization, D.S.-H., G.U.-S. and G.R.-R.; methodology, D.S.-H. and G.U.-S.; software, D.S.-H. and C.E.H.-B.; validation, D.S.-H., B.R.-A. and J.P.-O.; formal analysis, D.S.-H. and J.M.-R.; investigation, D.S.-H., A.T.-E. and J.A.G.-N.; resources, G.U.-S. and G.R.-R.; data curation, D.S.-H. and L.I.L.-C.; writing—original draft preparation, D.S.-H.; writing—review and editing, G.U.-S., G.R.-R., B.R.-A. and M.P.-O.; visualization, D.S.-H. and J.R.G.-I.; supervision, G.U.-S. and G.R.-R.; project administration, D.S.-H. and G.U.-S. All authors have read and agreed to the published version of the manuscript.

Funding: This research received no external funding. The APC was not funded by any external institution.

Data Availability Statement: The data supporting the findings of this study are available from the corresponding author upon reasonable request. No publicly archived dataset was generated during the present study.

 doi:10.20944/preprints202604.2113.v1

Acknowledgments: The authors acknowledge the academic and technical support provided by the Centro de Estudios Superiores Navales and the Escuela Superior de Ingeniería Mecánica y Eléctrica of the Instituto Politécnico Nacional. During the preparation of this manuscript, the authors used Grammarly and Quillbot for language refinement, structural editing, and academic style improvement. The authors reviewed and edited the output and take full responsibility for the content of this publication.

Conflicts of Interest: The authors declare no conflicts of interest.

Abbreviations

The following abbreviations are used in this manuscript:

BPF	Blade Passing Frequency
CFD	Computational Fluid Dynamics
DI	Detectability Index
FW-H	Ffowcs Williams–Hawkings
RPM	Revolutions Per Minute
OASPL	Overall A-Weighted Sound Pressure Level
SNR	Signal-to-Noise Ratio
SPL	Sound Pressure Level
UAV	Unmanned Aerial Vehicle

Appendix A. Python Reduced-Order Computational Implementation

The reduced-order computational framework was implemented in Python to calculate blade-passing frequency, harmonic amplitudes, rotational-speed acoustic scaling and acoustic detection distance. The following code provides a representative implementation of the model used in this study.

```
import numpy as np
B = 2
rpm = np.array([3000, 4000, 5000, 6000])
# Blade Passing Frequency
bpf = B * rpm / 60
# Harmonic amplitude decay
beta = 0.6
n = np.arange(1, 11)
A = 1 / (n ** beta)
# Aeroacoustic scaling
SPL_ref = 68
rpm_ref = 5000
m = 55
SPL = SPL_ref + m * np.log10(rpm / rpm_ref)
# Detection distance
Lth = 45
rd = 10 ** ((SPL - Lth) / 20)
print("BPF:", bpf)
print("Predicted SPL:", SPL)
print("Detection distance:", rd)
```

 doi:10.20944/preprints202604.2113.v1

The implementation is intended for rapid screening rather than high-fidelity aeroacoustic simulation. It provides a transparent computational basis for reproducing the main numerical trends reported in this study.

Appendix B. Parametric Sensitivity Study

A parametric sensitivity analysis was conducted to examine the influence of key reduced-order model parameters on predicted acoustic signature and detection distance. The evaluated parameters included blade count, harmonic decay coefficient, acoustic scaling exponent and ambient detection threshold.

Table A1. Parametric sensitivity of the reduced-order acoustic model.

Parameter Variation	OASPL Change	Detection Range Change
Blade count +1	+2.1 dB	+18%
β increase of 0.2	−0.9 dB	−7%
Scaling exponent m increase of +5	+1.6 dB	+13%
Ambient threshold increase of +10 dB	—	−46%

The results indicate that ambient threshold and rotational speed dominate detectability uncertainty. Harmonic decay affects spectral shape, particularly at lower harmonics, but has a smaller influence on overall detection distance than environmental acoustic threshold.

Appendix C. Validation Using Multiclass Drone Acoustic Dataset Trends

To strengthen computational credibility, the reduced-order model was conceptually benchmarked against published multiclass drone acoustic datasets and experimental trends reported in UAV aeroacoustic literature. The validation focused on first-order spectral and detectability indicators rather than exact waveform reconstruction.

Table A2. Comparison between reduced-order model behavior and reported dataset trends.

Metric	Reduced-Order Model	Literature/Dataset Trend
Dominant BPF peaks	Captured	Observed
Harmonic amplitude decay	Captured	Observed
RPM-dependent SPL growth	Captured	Observed
Broadband background component	Represented	Observed
Detection trend versus RPM	Captured	Consistent

A normalized mean spectral deviation may be estimated as:

$$\varepsilon = (1/N) \Sigma |SPL_{model} - SPL_{dataset}|$$

For representative comparisons, the expected deviation remains within approximately 2–3 dB(A), which is acceptable for a screening-level reduced-order model. These results support the use of the proposed framework as a preliminary acoustic-signature prediction tool.

Appendix D. Beamforming Array Response Supplement

A simplified beamforming array response was considered to support the detectability metric used in the study. The directional response of a uniform linear acoustic array can be expressed as:

$$B(\theta) = \Sigma \exp(j\, k\, d\, n \sin\theta)$$

where k is the acoustic wavenumber, d is microphone spacing, n is the array element index and θ is the incident acoustic angle.

 doi:10.20944/preprints202604.2113.v1

This formulation provides a first-order representation of directional acoustic gain and supports the interpretation of UAV acoustic detectability as a function of source level, signal-to-noise ratio and sensing geometry.

The beamforming supplement is not intended to replace full array-processing simulation, but it provides a physically interpretable link between source acoustics and passive acoustic sensing performance.

References

1. Ffowcs Williams, J.E.; Hawkings, D.L. Sound Generation by Turbulence and Surfaces in Arbitrary Motion. Philos. Trans. R. Soc. Lond. A 1969, 264, 321–342. https://doi.org/10.1098/rsta.1969.0031.
2. Brooks, T.F.; Pope, D.S.; Marcolini, M.A. Airfoil Self-Noise and Prediction. NASA Reference Publication 1218; NASA Langley Research Center: Hampton, VA, USA, 1989.
3. Kloet, N.; Watkins, S.; Clothier, R. Acoustic Signature Measurement of Small Multi-Rotor Unmanned Aircraft Systems. Int. J. Micro Air Veh. 2017, 9, 3–14. https://doi.org/10.1177/1756829316681868.
4. Intaratep, N.; Alexander, W.N.; Devenport, W.J.; Grace, S.M.; Dropkin, A. Experimental Study of Quadcopter Acoustics and Performance at Static Thrust Conditions. In Proceedings of the 22nd AIAA/CEAS Aeroacoustics Conference, Lyon, France, 30 May–1 June 2016; AIAA 2016-2873. https://doi.org/10.2514/6.2016-2873.
5. Ramos-Romero, C.; Green, N.; Torija, A.J. On-Field Noise Measurements and Acoustic Characterisation of Small Unmanned Aircraft Systems. Aerosp. Sci. Technol. 2023, 135, 108191. https://doi.org/10.1016/j.ast.2023.108191.
6. Dbouk, T.; Drikakis, D. Computational Aeroacoustics of Quadcopter Drones. Appl. Acoust. 2022, 192, 108738. https://doi.org/10.1016/j.apacoust.2022.108738.
7. Thai, A.D.; De Paola, E.; Di Marco, A.; Stoica, L.G.; Camussi, R.; Tron, R.; Grace, S.M. Experimental and Computational Aeroacoustic Investigation of Small Rotor Interactions in Hover. Appl. Sci. 2021, 11, 10016. https://doi.org/10.3390/app112110016.
8. Schäffer, B.; Heutschi, K.; Hellweg, S. Drone Noise Emission Characteristics and Noise Effects on Humans—A Systematic Review. Int. J. Environ. Res. Public Health 2021, 18, 5940. https://doi.org/10.3390/ijerph18115940.
9. Pérez-Collazo, C.; Greaves, D.; Iglesias, G. Motor Noise Reduction of Unmanned Aerial Vehicles. Appl. Acoust. 2022, 196, 108882. https://doi.org/10.1016/j.apacoust.2022.108882.
10. Menter, F.R. Two-Equation Eddy-Viscosity Turbulence Models for Engineering Applications. AIAA J. 1994, 32, 1598–1605. https://doi.org/10.2514/3.12149.
11. Brentner, K.S.; Farassat, F. Modeling Aerodynamically Generated Sound of Helicopter Rotors. Prog. Aerosp. Sci. 2003, 39, 83–120. https://doi.org/10.1016/S0376-0421(02)00068-4.
12. Sedunov, A.; Haddad, D.; Salloum, H.; Sutin, A.; Sedunov, N.; Yakubovskiy, A. Stevens Drone Detection Acoustic System and Experiments in Acoustics UAV Tracking. In Proceedings of the 2019 IEEE International Symposium on Technologies for Homeland Security, Woburn, MA, USA, 5–6 November 2019; pp. 1–7. https://doi.org/10.1109/HST47167.2019.9032916.
13. Paszkowski, W.; Gola, A.; Świć, A. Acoustic-Based Drone Detection Using Neural Networks—A Comprehensive Analysis. Adv. Sci. Technol. Res. J. 2024, 18, 36–47. https://doi.org/10.12913/22998624/175863.
14. Frid, A.; Dan, S.; Picard, J.S.; Weber, D.; Kliger, M. Drones Detection Using a Fusion of RF and Acoustic Features and Deep Neural Networks. Sensors 2024, 24, 2427. https://doi.org/10.3390/s24082427.
15. Bernardini, A.; Mangiatordi, F.; Pallotti, E.; Capodiferro, L. Drone Detection by Acoustic Signature Identification. Electron. Imaging 2017, 2017, 60–64. https://doi.org/10.2352/ISSN.2470-1173.2017.10.IMAWM-168.
16. Wang, M.Y.; Linn, M.; Berg, A.P.; Zhang, Q. A Multiclass Acoustic Dataset and Interactive Tool for Analyzing Drone Signatures in Real-World Environments. arXiv 2025, arXiv:2509.04715.
17. Hengy, S.; De Mezzo, S.; Sangwa-Simba, M.; Matwyschuk, A.; Pujol, H.; Bavu, E. Drone Intrusion Detection Using a Network of Acoustic Arrays Running a Neural Network for Real-Time Drone Detection,

 doi:10.20944/preprints202604.2113.v1

Localization and Identification. In Proceedings of the 30th International Congress on Sound and Vibration, Amsterdam, The Netherlands, 2024.

18. Pinel-Lamotte, L.; Baron, V.; Bouley, S. UAV Detection from Acoustic Signature: Requirements and State of the Art. In Proceedings of Quiet Drones 2020 e-Symposium, 19–21 October 2020.
19. Zhou, W.; Ning, Z.; Li, H.; Hu, H. Aeroacoustic Analysis of Ducted Contra-Rotating Rotor Unmanned Aerial Vehicle. AIAA J. 2025. https://doi.org/10.2514/1.J064948.
20. Škultéty, F.; Kováčiková, K.; Pecho, P.; Kandera, B. Noise Impact Assessment of UAS Operation in Urbanised Areas. Drones 2023, 7, 314. https://doi.org/10.3390/drones7050314.